Inorganic Chemistry

Article

pubs.acs.org/IC

Photon-Driven Reduction of Zn^{2+} to Zn Metal

Anthony C. Brooks, Katherine Basore, and Stefan Bernhard*

Department of Chemistry, Carnegie Mellon University, Pittsburgh, Pennsylvania 15213-3890, United States

ABSTRACT: Easily oxidized metals are of interest as a means of storing solar energy in the form of fuels. While their efficient metal/air batteries make them attractive solar fuel candidates, the photoreduction of the corresponding metal ions remains difficult. Accordingly, this work describes the photon driven reduction of Zn^{2+} by an iridium(III) photosensitizer (PS) and catalyst. $[Ir(ppy)_2(dtbbpy)](PF_6)$ (ppy = 2-phenylpyridine, dtbbpy = 4,4′-di-*tert*-butyl-2,2′-bipyridine) was found to be the most robust photocatalyst, and the use of $ZnCl_2$ as the Zn^{2+} starting material and acetonitrile as the solvent afforded the highest yield of Zn metal product. Under these conditions, a maximum of 430 catalyst turnover numbers were achieved. Cyclic voltammetry of $ZnCl_2$ in different solvents and of different zinc salts in acetonitrile (MeCN) demonstrated the roles of MeCN and Cl^- in the photoreduction mechanism. Kinetics measurements revealed a first order dependence of the initial rate on both $[Ir(ppy)_2(dtbbpy)](PF_6)$ and $ZnCl_2$. A first order decay of the reaction rate was also observed.

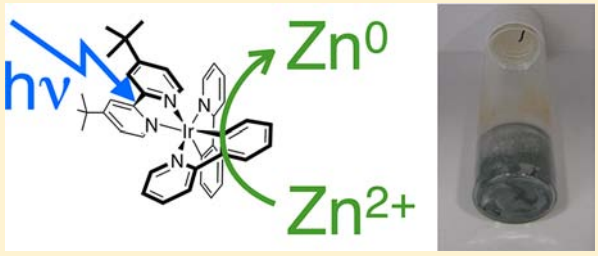

INTRODUCTION

Human energy consumption has been rising for decades. The resulting economic conditions and the environmental consequences of this growth will provide an opportunity for renewable energy applications to thrive. Many direct[1,2] and indirect[3] solar power conversion schemes are currently the subject of intense research, since they promise abundant energy that could potentially supplement or replace coal or petroleum on a massive scale.[4] Consequently, storing photon energy as chemical potential in solar fuels is of particular interest for replacing hydrocarbons for mobile applications. This approach alleviates the complications created by the seasonal and diurnal fluctuations commonly observed in solar energy conversion systems. Unlike photovoltaic energy, solar fuels are independent of the electrical grid, allowing them to be stored and transported easily as a mobile fuel. Specifically, H_2 is often identified as a promising candidate,[5,6] but storage requirements partially offset the high gravimetric energy densities desired for transportation applications. To illustrate, gaseous H_2 has a 39.4 kWh/kg theoretical specific energy density, but a safe, 700 bar tank system for mobile H_2 use has a theoretical specific energy density of 1.89 kWh/kg, which further drops because of losses from compression and fuel cell mass.[7]

Metals are an often-overlooked alternative to energy-dense liquid and gaseous solar fuels. Despite this oversight, zinc and aluminum are well suited for this application because they can utilize established Zn/air and Al/air batteries which are efficient, lightweight, and consume only these reactive metals and air. The very negative reduction potential of Al renders it an extremely efficient candidate for energy storage, but its reactivity will greatly complicate the photocatalytic production of this metal. Consequently, zinc is a more appealing prospect for a fuel cycle involving a mechanically rechargeable metal/air battery employing the relevant electrode reactions shown in Scheme 1.

Scheme 1. Redox Reactions Relevant to the Zn/Air Battery[a]

Anode:

$$Zn \longrightarrow Zn^{2+} + 2e^-$$
$$Zn^{2+} + 4OH^- \longrightarrow Zn(OH^-)_4^{2-}$$
$$Zn(OH^-)_4^{2-} \longrightarrow ZnO + H_2O + 2OH^-$$

Cathode:

$$O_2 + 2H_2O + 4e^- \longrightarrow 4OH^-$$

Overall reaction (E^0 = 1.65 V):

$$2Zn + O_2 \longrightarrow 2ZnO$$

[a]A strongly basic electrolyte is commonly used in these mechanically rechargeable fuel cells.

Neglecting the mass of the O_2 oxidant, zinc has a theoretical specific energy density of 1.35 kWh/kg.[8] Without the need for compression, only the battery is used for storage, which lowers the practical specific energy density just slightly to 1.084 kWh/kg.[9] The lightweight and remarkable 98% coulombic discharge efficiencies[10] of the Zn/air battery exemplify the great potential of zinc as a transportable, abundant solar fuel.

To make use of zinc as a renewable solar fuel, Zn^{2+} oxidized in the battery must be reduced back to Zn^0 by light. Also, a complementary reaction that oxidizes hydroxide ions to oxygen has to be driven by photons concomitantly. A robust and efficient photosensitizer (PS) responsible for the initial absorption of a photon is critical for such a scheme. Photoinduced electron transfer reactions will subsequently drive OH^- oxidation and Zn^{2+} reduction processes and thereby reverse the redox chemistry responsible for driving the Zn/air

Received: November 30, 2012
Published: May 6, 2013

   dx.doi.org/10.1021/ic302629q | *Inorg. Chem.* 2013, 52, 5794−5800

cell. Iridium complexes stand out as PSs because of their remarkable photophysical properties such as long lifetimes and photochemical robustness.[11] Furthermore, the highest occupied molecular orbital (HOMO) and the lowest unoccupied molecular orbital (LUMO) of cyclometalated iridium complexes can be tuned independently by modification of separate ligands, which allows the thermodynamics of electron transfer reactions to be fine-tuned.[12,13] Cyclometalated Ir(III) complexes are used in organic light-emitting diodes (OLEDs)[14] and as photocatalysts in many redox reactions including organic radical polymerizations,[15] cyclizations,[16] aldehyde fluoromethylations,[17] the water gas shift reaction,[18] and more prominently, the reduction of H_2O and CO_2 for solar fuels.[19,20] In H_2 evolving, water reduction reactions, turnover numbers (TONs, moles product/moles PS) of the Ir(III) PS have reached 10,000, which was achieved by the judicious design of the ligand sphere of these highly luminescent metal complexes.[21] The electrochemical and photochemical robustness of these phosphorescent materials is extraordinary and greatly facilitates the exploration of new photocatalytic systems relevant to the renewable energy field.

This work describes the visible-photon driven reduction of Zn^{2+} to Zn^0 (E_{red} = −0.76 V vs NHE) by an iridium(III) PS and catalyst system. To our knowledge, this is the first published case of the photocatalyzed reduction of a low redox potential metal ion by a transition metal complex. In being so, this initial work demonstrates the feasibility of Zn^{2+} reduction by a molecular photocatalyst for eventual use as a solar fuel. Contrasting, $[Ru(bpy)_3]^{2+}$ has been used to photoreduce Ag^+ to Ag metal,[22] but silver has a high work function, its cation is easy to reduce, and Ag^0 lacks the energy density necessary of a solar fuel. A dissimilar approach is the reduction of Zn^{2+} to Zn metal by solar thermal ZnO decomposition. At high temperatures achieved by concentrating sunlight, equilibrium shifts and ZnO splits into its elemental constituents O_2 and Zn.[23] Though ZnO splitting can occur at 1100 K, temperatures of 2300 K or higher are generally required, and low metal yields caused by the reoxidation of Zn^0 are commonly observed during cooling process.[24]

In this paper, $[Ir(ppy)_2(dtbbpy)]PF_6$ (ppy = 2-phenylpyridine, dtbbpy = 4,4′-di-*tert*-butyl-2,2′-bipyridine) is employed as a photocatalyst for the reduction of Zn^{2+}. Triethylamine (TEA) serves as a sacrificial electron donor for the aforementioned half reaction, an approach that is similar to work done by the hydrogen community while exploring water splitting systems.[25,26] While the use of ZnO as the Zn(II) source is preferential, ZnO is easily converted to $ZnCl_2$, so more important is the maintenance of charge balance. Like H_2 evolution systems, Zn^{2+} photoreduction ultimately requires a complementary oxidation half reaction, such as water oxidation, to maintain charge balance necessary for complete solar fuel photosynthesis. The structure−activity relationships of diverse Ir(III) PSs are explored, and rate studies revealed insights into the mechanistic details of these photocatalytic reduction reactions.

EXPERIMENTAL SECTION

All iridium complexes, including $[Ir(ppy)_2(dtbbpy)]PF_6$, were synthesized according to established procedures.[13,27] Acetonitrile was purchased from Fischer, triethylamine was purchased from Acros, and $ZnCl_2$ as well as the other zinc salts were obtained from Sigma. All chemicals were used as received.

Cyclic voltammetry was performed utilizing a CH instruments 600C electrochemical analyzer potentiostat. The setup employed a glassy carbon working, platinum counter, and silver wire pseudoreference electrode, against which a ferrocene internal standard was referenced at 0.380 V vs SCE.[28]

Photoreduction samples were prepared in 40 mL EPA vials with open top caps containing a fluoropolymer resin/silicone septa (ICHEM SB36-0040). A typical photoreaction contained 9 mL of acetonitrile, 1 mL of TEA, 1.1 μmol of $[Ir(ppy)_2(dtbbpy)]PF_6$, and 420 mg of $ZnCl_2$.

The samples were illuminated under argon in a custom designed, multiwell photoreactor: A 5 m long 24 W 460 nm LED strip with 300 diodes (Solid Apollo SA-LS-BL-3528-300-24 V) was mounted inside an 8 in. (203 mm) galvanized steel tube in a uniform, spiral pattern. The 60 mm high illumination zone was centered on the samples, which were magnetically stirred. Samples were held in place by a circular sample holder that was placed inside the steel tube. Sheaths were built by cutting transparent 1−1/4″ (31.8 mm) polycarbonate tube with a 1−1/8″ inner diameter into twelve 42 mm long pieces. Twelve of these short pieces were then mounted around a clear 3-1/2″ acrylic tube at a height of 40 mm. The septum covered EPA vials were used as illumination vessels. The sample holder was centered on a magnetic stirrer, and the distance between all the vials and the LED ribbon was uniformly kept at 28 mm. Before illumination, sample vials were degassed by cycling 6 times between vacuum and Ar atmosphere. Figure 1 depicts the photoreactor.

Figure 1. Custom designed photoreactor used in Zn^{2+} reducing photoreactions.

After illumination, the samples were purged with argon for 10 min to vacate any potential H_2 from the headspace. Quantitative conversion of reduced Zn^0 to H_2 was achieved by injecting photoreaction mixtures with 2 mL of concentrated hydrochloric acid, similar to the technique described by Vogel.[29]

The headspace of the acidified photoreduction vials was injected into a residual gas analyzer to permit calculation of total H_2 evolved by the procedure used by Curtin et al.[13] Catalytic TONs were calculated using the 1:1 stoichiometric ratio of H_2 to zinc product. In this case, because Zn^{2+} is reduced to Zn^0 and the Ir catalyst serves the dual function of PS, electron TONs are simply twice that of catalytic TONs. All TONs reported in this work are catalytic TONs.

X-ray diffraction was measured using a PANalytical X′Pert PRO diffraction system. To prepare the completed photoreduction samples for X-ray diffraction, the solution phase was extracted through the septum of the capped photoreduction vial to preserve the argon atmosphere in the headspace. MeCN was then added and extracted similarly and the samples were purged with argon until dry. The zinc product was then briefly exposed to air during transfer and diffraction measurement.

dx.doi.org/10.1021/ic302629q | Inorg. Chem. 2013, 52, 5794−5800

RESULTS AND DISCUSSION

Mixtures of $ZnCl_2$ in acetonitrile were observed to yield reduced Zn metal after illumination under visible light in the presence of an iridium(III) PS and triethylamine. Light, TEA, and the Ir PS all proved necessary; without any given component, no reduction of Zn^{2+} was observed. TEA is known to reductively quench an excited-state iridium PS.[30] The Ir(III) PS photocatalytically transfers the reducing equivalents from TEA to Zn^{2+}, yielding the reduced Zn metal product and oxidizing TEA.

The oxidation mechanism of TEA appears to be the same as in similar H_2 evolving systems, in which the two electron oxidation of TEA yields diethylamine and acetaldehyde.[25] This mechanism is confirmed by the failure of anhydrous $ZnCl_2$ to yield any reduced Zn metal; H_2O is required to produce acetaldehyde,[31] which is otherwise supplied by H_2O bound to the Zn salt crystal lattice. However, prior to the involvement of H_2O, the oxidation of TEA releases two protons.[25] Despite the influx of protons, there is no pH change over the course of a photoreduction. The protons released are effectively buffered by TEA, which outnumber Cl^- by a 7:2 excess in a typical photoreduction mixture. This ensures that the Zn^0 product will not be reoxidized and permits the involvement of free Cl^- in the Zn^{2+} reduction mechanism.

Several iridium(III) PSs were evaluated for their effectiveness in the reduction of Zn^{2+} to Zn^0. TONs of each Ir PS tested are shown in Figure 2. All Ir PSs demonstrated some degree of photocatalytic capacity, with the exception of $[Ir(ppy)_2(dppe)](PF_6)$. Presumably, $[Ir(ppy)_2(dppe)](PF_6)$ is ineffective because it luminesces from its π to π^* excited state; all other Ir PSs tested emit via triplet state metal to ligand charge transfer (^{3}MLCT) transitions.[27b] Though a dominant ^{3}MLCT proved necessary, there was little correlation between photocatalytic ability and any other photophysical properties of the Ir PS, including excited state lifetime, extinction coefficient at 465 nm, and emission wavelength. This stands in contrast to similar H_2O reducing systems previously studied by the Bernhard group,[25] which demonstrated a dependence of e^- TONs on the lifetime of the Ir PS. In the future, a better understanding of the photocatalytic mechanism should yield clearer insights into structure property relationships observed in Zn^{2+} photoreduction reactions. Among the Ir(III) complexes tested, $[Ir(ppy)_2(dtbbpy)](PF_6)$ yielded the highest TONs and was used in subsequent studies.

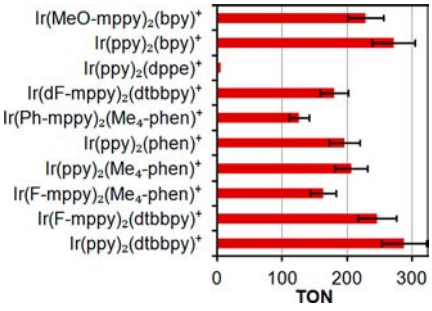

Figure 2. Catalytic TONs afforded by various iridium(III) PS complexes after 48 h illumination. A constant concentration of 110 μM and PF_6^- counterion to each Ir PS ensured direct comparison. Additionally, each Ir PS photoreduction mixture contained 9 mL of MeCN, 1 mL of TEA, and 420 mg of $ZnCl_2$. 95% percent confidence intervals are shown. The abbreviations for the ligands used are as follows: ppy: 2-phenylpyridine, F-mppy: 2-(4-fluorophenyl)-5-methylpyridine, dF-mppy: 2-(2,4-difluorophenyl)-5-methylpyridine, Ph-mppy: 2-([1,1′-biphenyl]-4-yl)-5-methylpyridine, MeO-mppy: 2-(4-methoxyphenyl)-5-methylpyridine, bpy: 2,2′-bipyridine, dtbbpy: 4,4′-di-*tert*-butyl-2,2′-bipyridine, phen: 1,10-phenanthroline, Me_4-phen: 3,4,7,8-tetramethyl-1,10-phenanthroline, dppe: (Z)-1,2-bis-(diphenylphosphino)ethane.

Although the photoreduction product possessed similar reactivity and appearance to Zn^0; X-ray diffraction (XRD) was utilized to confirm its identity as such. The measured XRD pattern is shown in Figure 3. Both the angle and relative intensities of the pattern obtained from the photoreduction product match reported literature values for Zn metal.[32] Excess zinc chloride was removed via MeCN rinses and was not detected. Minor peaks can be attributed to small quantities of zinc oxide formed by oxidation of the Zn^0 product during XRD sample processing, or by residual water and O_2 in the reaction vial. Importantly, the Zn metal analysis via H_2 evolution is not affected by ZnO, thus giving a true value for the yield of Zn^0 with or without ZnO present.

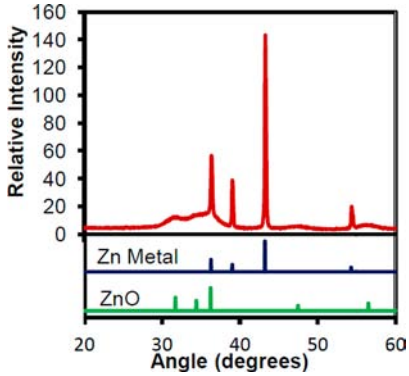

Figure 3. X-ray diffraction pattern of zinc product (red) with accepted literature patterns for Zn^0 (blue) and ZnO (green) shown underneath. The correspondence of the experimental peaks to Zn^0 confirms zinc metal as the major photoproduct. Θ−2Θ scan performed at 30 kV, 10 mA, from 20° to 60°.

The verification of Zn^0 as the photoreaction product allowed for the systematic optimization of the photocatalytic system. In addition to iridium PS tuning, studies were conducted varying the solvent, H_2O concentration, and zinc salt, with the best conditions from each experiment being used in the subsequent.

The use of different zinc salts as a Zn^{2+} source was found to have a significant effect on the TONs of the Ir(III) PS. Figure 4 shows the results of this study. While $ZnCl_2$ yielded the most reduced Zn^0, the most remarkable trend is the superior performance of ZnX_2 halide salts. Despite higher solubility, other salts afforded much less Zn^0 product. $Zn(BF_4)_2$ was the only salt that completely dissolved in the 1 TEA: 9 MeCN photoreaction solution, yet produced only 5 μmol of Zn^0 in photoreductions. This indicates that to some extent, the halide counterion remains coordinated to the Zn(II) reactant. Furthermore, it suggests halides may play a role in the reaction mechanism, aiding in Zn^{2+} reduction perhaps by stabilizing a Zn^+ intermediate.

The redox behavior of fully dissolved ZnI_2, $ZnCl_2$, and $ZnBr_2$ was examined through cyclic voltammetry in MeCN to determine if reduction potential correlated with yield of Zn^0. These results are shown in Figure 5. In theory, a less negative reduction potential of the ZnX_2 salt would indicate a greater

dx.doi.org/10.1021/ic302629q | Inorg. Chem. 2013, 52, 5794−5800

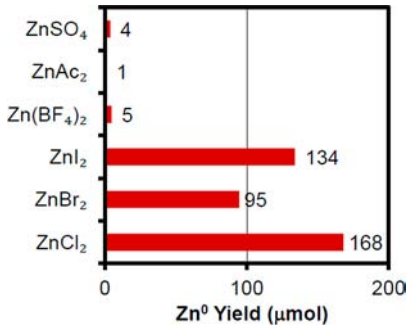

Figure 4. TONs of $[Ir(ppy)_2(dtbbpy)](PF_6)$ in the reduction of various Zn(II) salts to Zn^0. Each photoreduction mixture contained 9 mL of MeCN, 1 mL of TEA and 110 μM $[Ir(ppy)_2(dtbbpy)](PF_6)$ in addition to 2.01 mmol of the given Zn(II) salt.

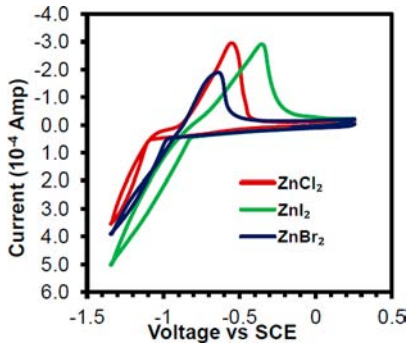

Figure 5. Cyclic voltammograms of $ZnCl_2$ (red), ZnI_2 (green), and $ZnBr_2$ (blue). MeCN and 0.1 M tetrabutylammonium hexafluorophosphate ($TBAPF_6$) served as solvent and electrolyte, at a scan rate of 0.1 V/s.

thermodynamic driving force and thus more TONs in reduction to Zn^0 by an Ir PS. However, no correlation can be found between reduction potential of ZnX_2 from Figure 5 and yield of Zn^0 in Figure 4.

This lack of correlation could be explained by different mechanisms of Zn^{2+} reduction by CV and by an Ir(III) PS. Figure 5 shows no sign of Zn^+, a highly unstable species. The reduction of Zn^{2+} to Zn^0 by CV is a simultaneous 2 electron transfer; Zn(II) is reduced directly to zinc metal. This differs from the accepted method of reduction by a heteroleptic Ir(III) PS, which was shown to reduce H_2O in a similar system by consecutive transfers of a single electron.[13,33] The possible involvement of any Ir(I) species can be excluded because it is not observed electrochemically within the potential window of this study. The bpy and then ppy ligands are reduced first, and catalysis by iridium complexes has been shown to involve a singly reduced $[Ir(C^N)_2(N^N)]^0$ species that is characterized by e^- population of the π^* orbital of the diimine ligand.[25] The lifetime of Zn^+ would be short, but relatively stable Zn(I) compounds are known to exist as diamagnetic Zn_2^{2+} species, which bind an array of bridging ligands to form dinuclear complexes.[34] A longer lived Zn^+ species stabilized by a halide ligand could explain how a 2 e^- redox reaction could be driven photochemically by an Ir(III) PS. Halides are also known for their bridging capabilities, and $ZnCl_2$ is thought to stabilize Zn_2^{2+}, something that would also increase TONs in an environment in which two proximal Zn^+ ions would be likely to disproportionate.[35]

Similar to the zinc salt study, the photocatalytic ability of the $[Ir(ppy)_2(dtbbpy)](PF_6)$ catalyst was tested in different solvents to further optimize its performance. TONs of the Ir PS were maximized in acetonitrile as the solvent (9 mL MeCN:1 mL TEA); 289 were achieved after 3 days. The observation that zinc chloride had neither the highest nor lowest solubility in MeCN prompted the addition of MeCN to other solvent bodies. Even as the minority component in other solvents (1 mL MeCN:8 mL solvent:1 mL TEA), the addition of MeCN increased TONs substantially, as Figure 6 demonstrates.

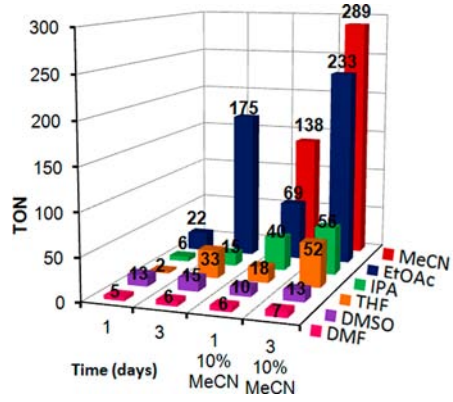

Figure 6. $[Ir(ppy)_2(dtbbpy)](PF_6)$ TONs in solvent bodies of varied compositions. Photoreduction mixtures "w/MeCN" contained 1 mL of TEA, 1 mL of MeCN, and 8 mL of solvent. Other photoreactions lacked MeCN and contained 1 mL of TEA, 9 mL of solvent. The samples were 110 μM in Ir PS and contained 420 mg of $ZnCl_2$.

These results indicate that MeCN may yield higher TONs because of a participation in the reaction mechanism, and that it does not play an innocent role in the greater solvent body. In small quantities, MeCN could still form part of the inner solvation shell or coordinate directly to a zinc species. It is unlikely that MeCN interacts directly with the Ir PS to produce such results; Ir(III) complexes have shown greater capacity to photoreduce H_2O in other solvents.[25]

Cyclic voltammetry was performed to test whether the effect of acetonitrile on TONs observed in Figure 6 is a result of a shift in the reduction potential of $ZnCl_2$. Electrochemistry experiments were performed at low $ZnCl_2$ concentrations, well within its solubility limit in tetrahydrofuran (THF) and MeCN. Figure 7 shows two dramatically different cyclic voltammo-

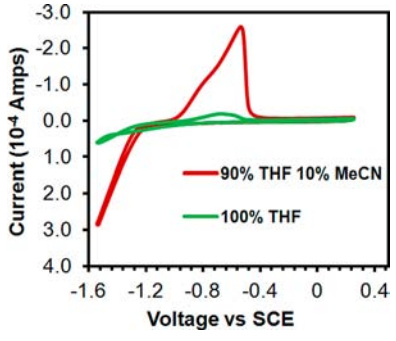

Figure 7. Cyclic voltammograms of $ZnCl_2$ in pure THF and in THF with 10% acetonitrile v/v. The scan rate was 0.1 V/s and 0.1 M $TBAPF_6$ served as the electrolyte.

dx.doi.org/10.1021/ic302629q | Inorg. Chem. 2013, 52, 5794−5800

grams of $ZnCl_2$ in THF with and without 10% v/v MeCN. The scan in pure THF exhibits only slight reduction of Zn^{2+} and bears little resemblance to the scan of $ZnCl_2$ in MeCN depicted in Figure 5. Conversely, upon the addition of 10% MeCN, there is both a positive potential shift and increase in the reduction of Zn^{2+}, as well as a strong resemblance to the $ZnCl_2$ CV scan in Figure 5. Addition of H_2O reveals a dominating water reduction peak at less negative voltages before the onset of zinc reduction, thus obscuring the Zn(II) reduction peak and making it difficult to determine the effect of H_2O on the reduction potential of Zn(II).

These results reinforce the hypothesis that acetonitrile interacts closely with Zn^{2+} in its reduction mechanism. The increased reduction potential of $ZnCl_2$ upon addition of MeCN to THF explains the increased TONs under these conditions, and also presumably the similar effect observed in other solvents that were not suitable for CV measurements. Furthermore, the success of small parts MeCN in yielding high TONs allows for the possibility of utilizing a more benign solvent to improve environmental impact while preserving high Zn^0 yields. It is noteworthy that TONs increase as the potential difference between the onset of Zn^{2+} reduction and the reduction potential of $[Ir(ppy)_2(dtbbpy)](PF_6)$ (E_{red} = −1.18 V vs SHE[27a]) grows. This energy difference is ultimately responsible for driving the reaction.

Along the same lines, water was added to the photoreduction solvent body to investigate its effect on the catalytic system. Small quantities of water, down to 50 μL/10 mL photoreduction vial, inhibited the ability of $[Ir(ppy)_2(dtbbpy)](PF_6)$ to reduce Zn^{2+}. The concurrent production of H_2 was also measured, both of which are shown in Figure 8. The gradual

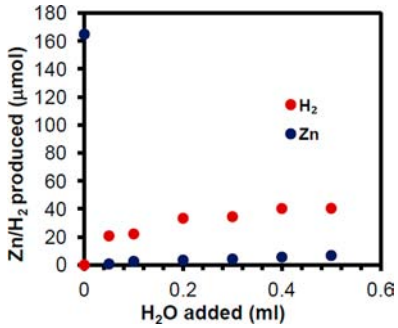

Figure 8. Dependence of Zn^0 and H_2 yields on H_2O volume in reaction mixture. Photoreduction mixtures contained 110 μmol $[Ir(ppy)_2(dtbbpy)](PF_6)$, 420 mg of $ZnCl_2$, 1 mL of TEA, H_2O, and enough MeCN to bring to volume (10 mL total).

rise in H_2 production indicates that the steep drop of Zn^0 production is not the result of competitive inhibition. Instead, H_2O must play an active role in inhibiting the reduction of Zn^{2+}.

Given the affinity of H_2O for Zn^{2+}, the addition of water would readily displace a relatively weak acetonitrile ligand bound to a zinc ion. This explanation is consistent with the mechanism postulated previously that the coordination of MeCN to zinc is required for the photoreduction of Zn^{2+}. It also supports the CV evidence which indicated that the reduction of water occurs at less negative potentials than the reduction of Zn^{2+}. In fact, dominance of acetonitrile ligands in the coordination environment of the ionic zinc species is further supported by excluding the possibility of any TEA-Zn(II) interaction. Proton NMR studies revealed that the addition of $ZnCl_2$ to a TEA solution in acetonitrile failed to shift TEA peaks, indicating a lack of coordination of the amine to Zn^{2+}.

To further elucidate the mechanism of Zn^{2+} photoreduction by an Ir PS, several kinetics experiments were performed. First, the photoreduction rate was measured and analyzed, with the results displayed in Figure 9. After 100 h, the Zn^0 production had mostly ceased, and the experimental data demonstrates a strong fit with first order rate decay.

While the decreased reaction rate over time could be attributed to the consumption of $ZnCl_2$ starting material or decay of the Ir(III) PS, the latter appears more likely. Before the illumination of the photoreductions, $[Ir(ppy)_2(dtbbpy)](PF_6)$ is completely dissolved but $ZnCl_2$ is saturated. If the first order kinetics observed were a result of a decrease in dissolved Zn^{2+}, a longer initial constant rate would be expected in Figure 9 because of $ZnCl_2$ saturation. In the case of a heterogeneous reaction, more complicated kinetics would be expected. Conversely, first order deterioration of cyclometalated Ir(III) PS have been observed in similar H_2 systems by the dissociation of the bipyridine ligand.[36]

Ten days of illumination yielded an average of 473 μmol Zn^0 product (same conditions, not shown in Figure 9). Using 473 μmol as the maximum yield of Zn^0, the linearized kinetic first order decay model showed a good fit. The high R^2 value confirms the first order catalytic process observed in this system. 473 μmol Zn^0 is equivalent to 430 TONs of $[Ir(ppy)_2(dtbbpy)](PF_6)$, which is the highest TON value reported in this work.

Kinetics experiments examining the dependence of the initial rate on Ir PS concentration were also performed. To achieve this, Zn^0 yields were repeatedly measured at 1, 2, 4, and 8 h for each concentration of Ir(III) PS. The slopes of the lines generated represent the initial reaction rate, which in turn were plotted against concentration of the Ir PS, shown in Figure 10. The resulting linear graph indicates a first order dependence of initial rate with respect to catalyst concentration. This dependence is consistent both with consecutive one electron transfers to produce Zn^0 via Zn^+, or single electron transfers to two separate Zn^{2+} species and subsequent disproportionation between two Zn^+ ions.

Similar initial rate experiments were conducted to determine the dependence of the initial rate on the mass of $ZnCl_2$ added to photoreductions. The plot of initial rate vs $ZnCl_2$ mass concentration can be seen in Figure 11. Mass concentration is used because of saturation of the photoreduction mixture. The linear graph again indicates a first order dependence, though these results are difficult to interpret given that the $ZnCl_2$ is not completely dissolved and that Cl^- and Zn^{2+} both participate in the reaction mechanism. Furthermore, the positive x intercept raises questions as to the nature of the Zn^{2+} species reduced. These results are difficult to interpret and do not unambiguously identify the reaction mechanism, but the saturated photoreduction mixtures and the apparent existence of a minimum required $ZnCl_2$ concentration engender the possibility that the photoreduction of Zn^{2+} is heterogeneous.

■ CONCLUSION

The photon driven reduction of Zn^{2+} by an iridium(III) PS and catalyst is described. TONs of the Ir PS were systematically optimized through Ir ligand tuning, variation of solvent and zinc salt, as well as by the exclusion of H_2O. In conditions

dx.doi.org/10.1021/ic302629q | Inorg. Chem. 2013, 52, 5794−5800

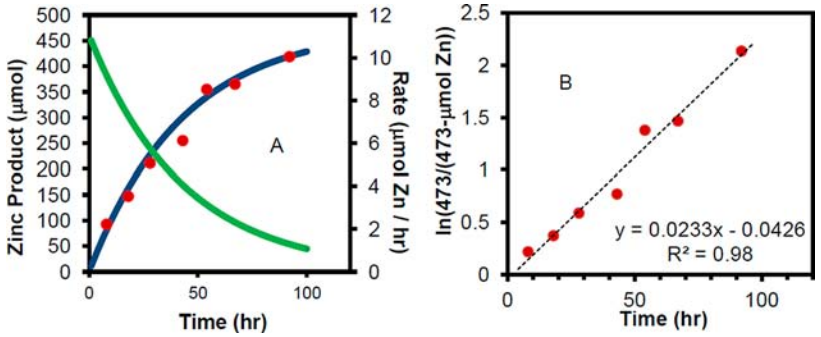

Figure 9. Measured Zn^0 production with respect to time (red), the optimal kinetic trace for first order rate decay (blue), and rate of reaction (green). Reaction conditions were 1 mL of TEA, 9 mL of MeCN, 420 mg of $ZnCl_2$, and 110 μM $Ir(ppy)_2(dtbbpy)](PF_6)$ per vial (A). Linearized experimental data and kinetic model of first order decay, adapted from data shown in Figure 9A (B).

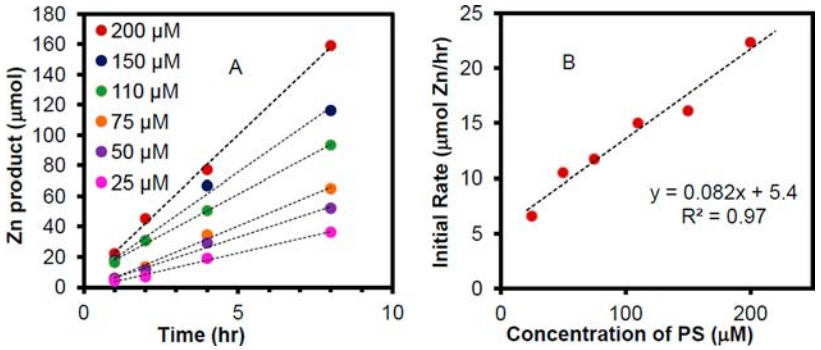

Figure 10. Initial steady-state zinc production at various concentrations of $[Ir(ppy)_2(dtbbpy)](PF_6)$. Each photoreduction mixture contained 1 mL of TEA, 9 mL of MeCN, 420 mg of $ZnCl_2$, and the Ir PS (A). First order kinetic dependence of the initial reaction rate on concentration of the $[Ir(ppy)_2(dtbbpy)](PF_6)$ PS. Each data point is an average of 4 samples (B).

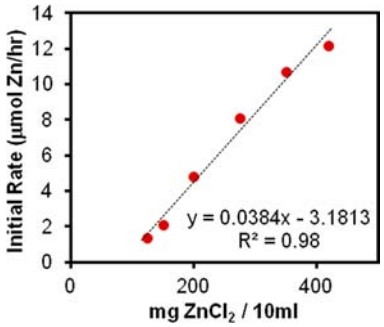

Figure 11. Kinetic dependence of initial reaction rate on the mass concentration of $ZnCl_2$ in heterogeneous photoreductions. Reaction conditions were 1 mL of TEA, 9 mL of MeCN, specified mass of $ZnCl_2$, and 110 μM $[Ir(ppy)_2(dtbbpy)](PF_6)$ per vial.

employing $[Ir(ppy)_2(dtbbpy)](PF_6)$ as the PS, $ZnCl_2$, and pure acetonitrile solvent, a maximum of 430 turnovers were achieved. Cyclic voltammetry was used to help elucidate the reaction mechanism, which appears to involve acetonitrile coordination to Zn^{2+} and the stabilization of a Zn^+ intermediate by a halide X^- from the starting material ZnX_2.

Kinetics measurements revealed a first order dependence of the initial rate on the Ir(III) PS, suggesting that each Ir PS will twice absorb a photon and transfer an electron per Zn^{2+} ion reduced. Additionally, a first order dependence on $ZnCl_2$ and a first order decay of reaction rate was found. These results offer a proof of concept for the reduction of Zn^{2+} by a molecular catalyst as well as a basis of understanding of the photoreduction mechanism, allowing for further optimization of and investigation into such a catalytic system.

AUTHOR INFORMATION

Corresponding Author

*E-mail: bern@cmu.edu.

Notes

The authors declare no competing financial interest.

ACKNOWLEDGMENTS

The authors acknowledges support from the National Science Foundation through CHE-1055547 and the Princeton MRSEC Grant DMR-0819860. Dr. Paul Salvador and Yiling Zhang of Carnegie Mellon Materials Science and Engineering performed the XRD measurement, which is greatly appreciated. The authors thank Kristen Hadley for assistance in hydrogen evolution experiments.

REFERENCES

(1) Brabec, C.; Gowrisanker, S.; Halls, J. M. M.; Laird, D.; Jia, S. J.; Williams, S. P. *Adv. Mater.* **2010**, *22*, 3839−3856.

(2) Hagfeldt, A.; Boschloo, G.; Sun, L. C.; Kloo, L.; Pettersson, H. *Chem. Rev.* **2010**, *110*, 6595−6663.

(3) Kraemer, D.; Poudel, B.; Feng, H. P.; Cavlor, J. C.; Yu, B.; Yan, X.; Ma, Y.; Wang, X. W.; Wang, D. Z.; Muto, A.; McEnaney, K.; Chiesa, M.; Ren, Z. F.; Chen, G. *Nat. Mater.* **2011**, *10*, 532−538.

(4) McDaniel, N. D.; Bernhard, S. *Dalton Trans.* **2010**, *39*, 10021−10030.

(5) Chen, X. B.; Shen, S. H.; Guo, L. J.; Mao, S. S. *Chem. Rev.* **2010**, *110*, 6503−6570.

dx.doi.org/10.1021/ic302629q | *Inorg. Chem.* 2013, 52, 5794−5800

(6) Andreiadis, E. S.; Chavarot-Kerlidou, M.; Fontecave, M.; Artero, V. *Photochem. Photobiol.* **2011**, *87*, 946−964.
(7) Fichtner, M. *J. Alloys Compd.* **2011**, *509*, S529−S532.
(8) Beck, F.; Rüetschi, P. *Electrochim. Acta* **2000**, *45*, 2467−2482.
(9) Lee, J.-S.; Tai Kim, S.; Cao, R.; Choi, N.-S.; Liu, M.; Lee, K. T.; Cho, J. *Adv. Energy Mater.* **2011**, *1*, 34−50.
(10) Wen, Y.-H.; Cheng, S.-Q.; Yang, Y.-S. *J. Power Sources* **2009**, *188*, 301−307.
(11) Flamigni, L.; Barbieri, A.; Sabatini, C.; Ventura, B.; Barigelletti, F. *Top. Curr. Chem.* **2007**, *281*, 143−203.
(12) Yuan, Y.-J.; Zhang, J.-Y.; Yu, Z.-T.; Feng, J.-Y.; Luo, W.-J.; Ye, J.-H.; Zou, Z.-G. *Inorg. Chem.* **2012**, *51*, 4123−4133.
(13) Curtin, P. N.; Tinker, L. L.; Burgess, C. M.; Cline, E. D.; Bernhard, S. *Inorg. Chem.* **2009**, *48*, 10498−10506.
(14) Baranoff, E.; Yum, J.-H.; Graetzel, M.; Nazeeruddin, M. K. *J. Organomet. Chem.* **2009**, *694*, 2661−2670.
(15) Lalevee, J.; Tehfe, M. A.; Dumur, F.; Gigmes, D.; Blanchard, N.; Morlet-Savary, F.; Fouassier, J. P. *ACS Macro Lett.* **2012**, *1*, 286−290.
(16) Tucker, J. W.; Nguyen, J. D.; Narayanam, J. M. R.; Krabbe, S. W.; Stephenson, C. R. *J. Chem. Commun.* **2010**, *46*, 4985−4987.
(17) Nagib, D. A.; Scott, M. E.; MacMillan, D. W. C. *J. Am. Chem. Soc.* **2009**, *131*, 10875−10877.
(18) Ziessel, R. *J. Am. Chem. Soc.* **1993**, *115*, 118−127.
(19) Metz, S.; Bernhard, S. *Chem. Commun.* **2010**, *46*, 7551−7553.
(20) Kang, P.; Cheng, C.; Chen, Z.; Schauer, C. K.; Meyer, T. J.; Brookhart, M. *J. Am. Chem. Soc.* **2012**, *134*, 5500−5503.
(21) DiSalle, B. F.; Bernhard, S. *J. Am. Chem. Soc.* **2011**, *133*, 11819−11821.
(22) Whitten, D. G. *Acc. Chem. Res.* **1980**, *13*, 83−90.
(23) Abanades, S.; Charvin, P.; Flamant, G. *Chem. Eng. Sci.* **2007**, *62*, 6323−6333.
(24) Keunecke, M.; Meier, A.; Palumbo, R. *Chem. Eng. Sci.* **2004**, *59*, 2695−2704.
(25) Cline, E.; Adamson, S.; Bernhard, S. *Inorg. Chem.* **2008**, *47*, 10378−10388.
(26) Han, Z.; McNamara, W. R.; Eum, M.-S.; Holland, P. L.; Eisenberg, R. *Angew. Chem., Int. Ed.* **2012**, *51*, 1667−16670.
(27) (a) Slinker, J. D.; Gorodetsky, A. A.; Lowry, M. S.; Wang, J. J.; Parker, S.; Rohl, R.; Bernhard, S.; Malliaras, G. G. *J. Am. Chem. Soc.* **2004**, *126*, 2763−2767. (b) Lowry, M. S.; Hudson, W. R.; Pascal, R. A.; Bernhard, S. *J. Am. Chem. Soc.* **2004**, *126*, 14129−14135. (c) Goldsmith, J. I.; Hudson, W. R.; Lowry, M. S.; Anderson, T. H.; Bernhard, S. *J. Am. Chem. Soc.* **2005**, *127*, 7502−7510.
(28) Pavlishchuk, V. V.; Addison, A. W. *Inorg. Chim. Acta* **2000**, *298*, 97−102.
(29) Vogel, A. L. *A Textbook of Quantitative Inorganic Analysis*; Logmans, Green and Co Ltd: London, U.K., 1951; Vol. *2*.
(30) Zhang, P.; Jacques, P.-A.; Chavarot-Kerlidou, M.; Wang, M.; Sun, L.; Fontecave, M.; Artero, V. *Inorg. Chem.* **2012**, *51*, 2115−2120.
(31) Chow, Y. L.; Danen, W. C.; Nelsen, S. F.; Rosenblatt, D. H. *Chem. Rev.* **1978**, *78*, 243−274.
(32) (a) Swanson, H. E.; Tatge, E. *Natl. Bur. Stand. Circ. (U. S.)* **1953**, *539*, 95. (b) Garcia-Martinez, O.; Rojas, R. M.; Vila, E.; de Vidales, J. L. M. *Solid State Ionics* **1993**, *63*, 442−449.
(33) Gärtner, F.; Denurra, S.; Losse, S.; Neubauer, A.; Boddien, A.; Gopinathan, A.; Spannenberg, A.; Junge, H.; Lochbrunner, S.; Blug, M.; Hoch, S.; Busse, J.; Gladiali, S.; Beller, M. *Chem.—Eur. J.* **2012**, *18*, 3220−3225.
(34) (a) Resa, I.; Carmona, E.; Gutierrez-Puebla, E.; Monge, A. *Science* **2004**, *305*, 1136−1138. (b) Li, T.; Schulz, S.; Roesky, P. W. *Chem. Soc. Rev.* **2012**, *41*, 3759−3771.
(35) Kerridge, B. D. H.; Tariq, S. A. *J. Chem. Soc. A* **1969**, 1122−1125.
(36) Tinker, L. L.; McDaniel, N. D.; Curtin, P. N.; Smith, C. K.; Ireland, M. J.; Bernhard, S. *Chem.—Eur. J.* **2007**, *13*, 8726−8732.